

Investigating the effect of atmospheric turbulence on mid-IR data quality with VISIR

Mario E. van den Ancker^a, Daniel Asmus^b, Christian Hummel^a, Hans-Ulrich Käuff^a, Florian Kerber^a, Alain Smette^b, Julian Taylor^a, Konrad Tristram^b, Jakob Vinther^a, and Burkhard Wolff^a

^aEuropean Southern Observatory, Karl-Schwarzschild-Strasse 2, D-85748 Garching bei München, Germany

^bEuropean Southern Observatory, Alonso de Córdova 3107, Vitacura, Casilla 19001, Santiago de Chile, Chile

ABSTRACT

A comparison of the FWHM of standard stars observed with VISIR, the mid-IR imager and spectrometer at ESO's VLT, with expectations for the achieved mid-IR Image Quality based on the optical seeing and the wavelength-dependence of atmospheric turbulence, shows that for N -band data ($7\text{--}12\mu\text{m}$), VISIR realizes an image quality about $0.1''$ worse than expected based on the optical seeing. This difference is large compared to the median N -band image quality of $0.3\text{--}0.4''$ achieved by VISIR. We also note that other mid-IR ground-based imagers show similar image quality in the N -band. We attribute this difference to an under-estimate of the effect of the atmosphere in the mid-IR in the parameters adopted so far for the extrapolation of optical to mid-IR seeing. Adopting an average outer length-scale of the atmospheric turbulence above Paranal $L_0 = 46$ m (instead of the previously used $L_0 = 23$ m) improves the agreement between predicted and achieved image quality in the mid-IR while only having a modest effect on the predicted image quality at shorter wavelengths (although a significant amount of scatter remains, suggesting that l_0 may not be constant in time). We therefore advocate adopting $L_0 = 46$ m for the average outer length scale of atmospheric turbulence above Cerro Paranal for real-time scheduling of observations on VLT UT3 (Melipal).

Keywords: Atmospheric Turbulence, Cerro Paranal, Image Quality, Infrared Astronomy, Seeing, VISIR

1. INTRODUCTION

Image Quality (hereafter IQ) – typically taken as the FWHM of an unresolved point-source – is one of the most important characteristics of an astronomical image. It is related, but not identical, to the astronomical seeing, commonly measured in the optical by either a differential image motion monitor (DIMM), or directly obtained at the focal plane of the telescope by measuring the movement of the telescope guide star on the guiding camera. An accurate prediction of image quality from a given seeing is an important element of both the simulation of an astronomical observation by ESO's Exposure Time Calculators (ETCs) and the short-term scheduling of observations done by ESO's Observing Tool (OT).

The accuracy of the conversion from optical seeing to image quality gained importance in ESO period 96 (the period starting on October 1st, 2015), as the constraints given by the user in their Phase 1 proposal are now taken as optical seeing, whereas prior to period 96, they were taken as the image quality at the observing wavelength. Short-term scheduling of observations conducted in service-mode also changed on October 1st: whereas before this date, filtering in the Observing Tool (OT) was done based on the measured image quality at the observing wavelength (in the case of VISIR from observations of standard stars), it is now done based on the optical seeing, converted to an expected image quality at the observing wavelength. The difference between optical seeing and

Further author information: (Send correspondence to M.v.d.A.)

M.v.d.A.: E-mail: mvandena@eso.org, Telephone: +49 89 3200660

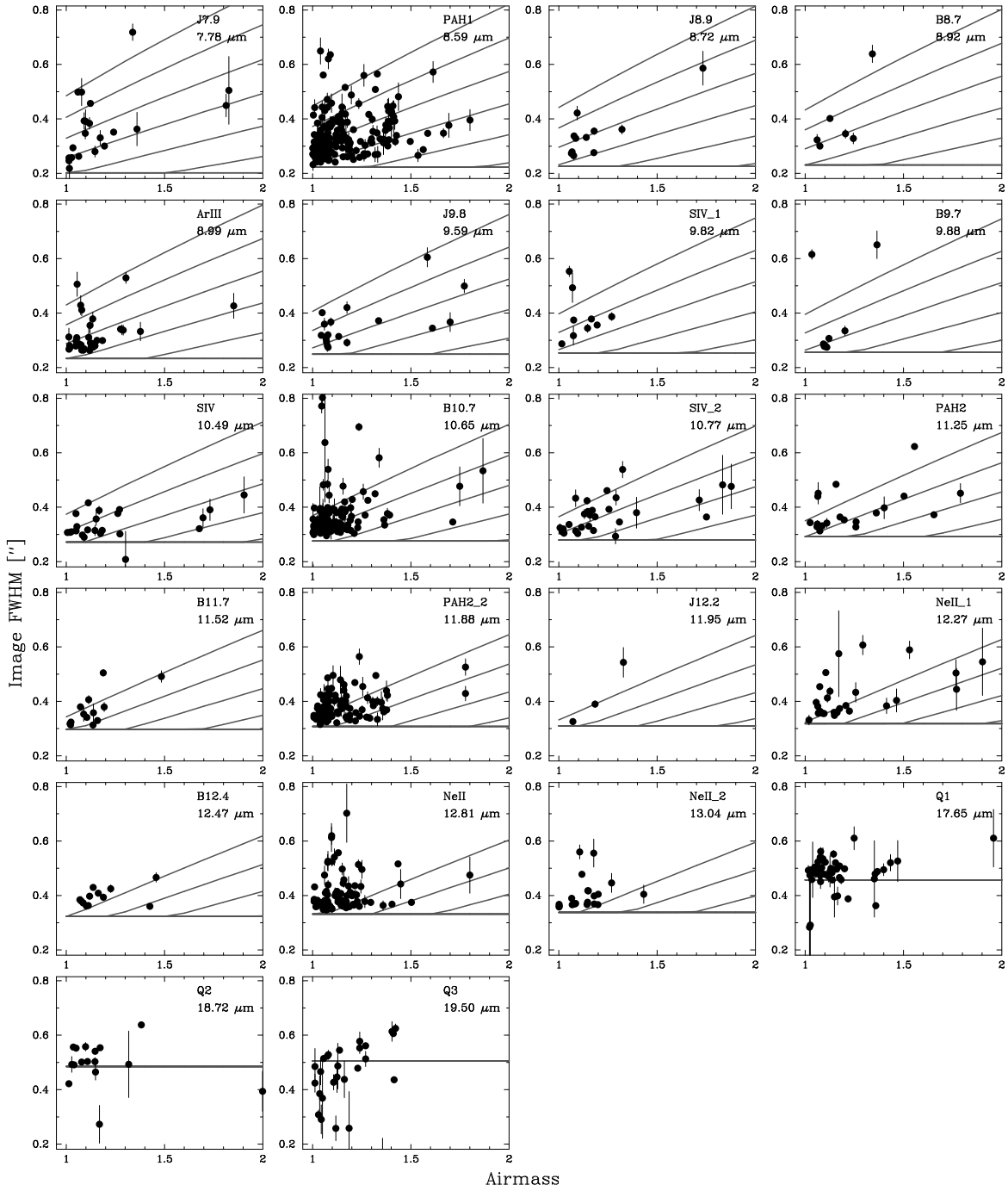


Figure 1. Achieved Image Quality as a function of airmass for VISIR standard stars observed between March 1 and October 20, 2015. In each plot the lines show the predicted behaviour for an optical seeing of (from top to bottom) 2.0, 1.8, 1.6, 1.4, 1.2, 1.0, 0.8, 0.6, and 0.4".

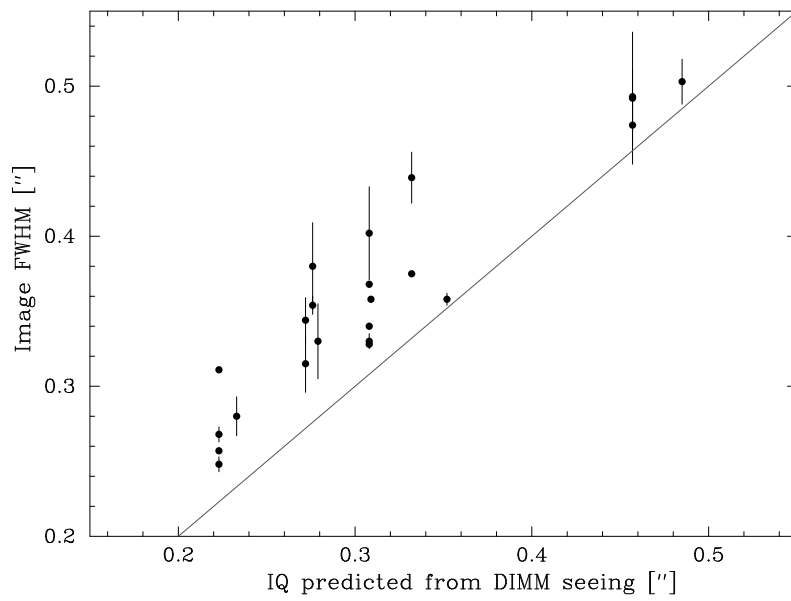
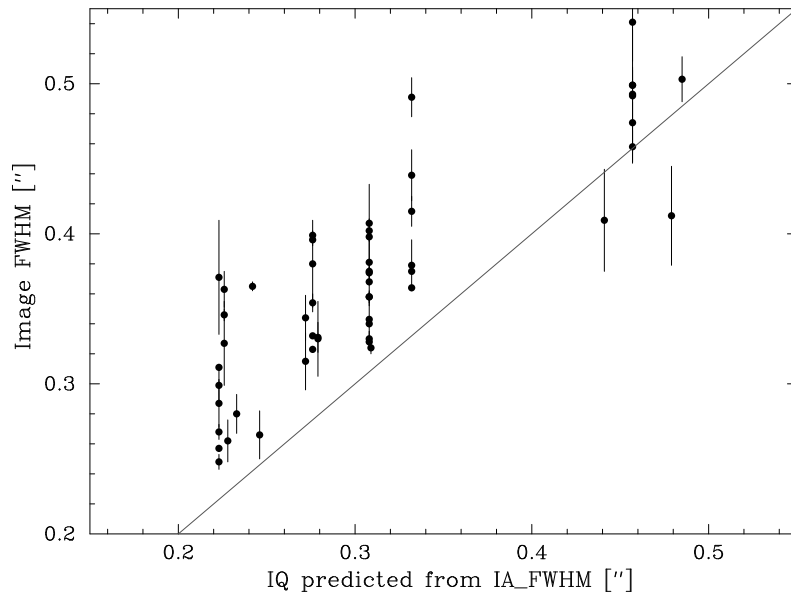


Figure 2. Comparison of achieved versus predicted image quality using IA_FWHM (“telescope” seeing) (top) and predicted image quality versus DIMM seeing (bottom). The solid line indicates achieved IQ = predicted IQ.

image quality is largest for instruments observing at wavelengths distant from the 500 nm reference wavelength for optical seeing, such as VISIR, the mid-IR imager and spectrograph on ESO’s VLT.

Given the potentially large effects on scheduling and executability of service-mode Observing Blocks we investigate in these proceedings the relation between image quality achieved in the mid-IR with VISIR, and the predictions from the VISIR ETC, and the implications for scheduling VISIR service-mode OBs.

2. IMAGE QUALITY MODEL IMPLEMENTED IN THE ETC

The VISIR Exposure Time Calculators* use the equations given in Reference 1 to compute the image quality at the central wavelength of a variety of VISIR filters with optical seeing and airmass as input parameters. The combined image quality is the quadratic sum of contributions due to the earth’s atmosphere, the diffraction limit of the telescope, and the transfer function of the instrument (taken to be 0.01” for VISIR):

$$IQ = \sqrt{FWHM_{atm}^2(s, x, \lambda) + FWHM_{tel}^2(D, \lambda) + FWHM_{ins}^2} \quad (1)$$

with s = seeing, λ = wavelength, x = airmass and D = telescope diameter.

For the atmospheric contribution to image quality we use

$$FWHM_{atm}(s, x, \lambda) = s \times x^{0.6} \times (\lambda/500nm)^{-0.2} \times \sqrt{1 + F_{Kolb} \times 2.183 \times (r_0/L_0)^{0.356}} \quad (2)$$

where L_0 is the wave-front outer-scale (set to 23 m; a value of infinity for L_0 corresponds to the case of pure Kolomogorov turbulence), and r_0 is the Fried parameter at the requested wavelength and airmass:

$$r_0 = 0.976 \times 500.0 \times 10^{-9}nm/s \times (180/\pi \times 3600) \times (\lambda/500.0nm)^{1.2} \times x^{-0.6} \quad (3)$$

and the Kolb factor

$$F_{Kolb} = 1/(1 + 300 \times D/L_0) - 1 \quad (4)$$

If the argument of the square root $\sqrt{1 + F_{Kolb} \times 2.183 \times (r_0/L_0)^{0.356}}$ is less than 0, the value of $FWHM_{atm}$ is set to 0.0.

We note that in the study by Martinez et al. the above equations were only compared to observed image quality at wavelengths ranging from the U band (0.36 μ m) to M (4.5 μ m). Their validity has so far not been investigated at longer wavelengths.

3. COMPARISON OF PREDICTED AND MEASURED IMAGE QUALITY

Observations of photometric standard stars are obtained several times per night with VISIR as part of the standard calibration plan for imaging observations taken in service-mode. These images are reduced by the VISIR pipeline, and used to obtain the conversion factor for photometry. In addition, the pipeline measures the FWHM in the x and y directions of the different beams of the perpendicular chop/nod pattern. These values are stored in the Quality Control database.† For data obtained after October 1st, 2015, this database also contains the optical seeing, as reported by the Differential Image Motion Monitor (DIMM), installed on Paranal, and the FWHM of the image recorded by the active optics analysis of the telescope (“guide probe seeing”).

In our analysis we limit ourselves to data obtained between March 1st and October 31th, 2015. This time interval covers only data taken after the VISIR upgrade,^{2,3} so older data (which may have been affected by known image quality issues prior to the upgrade) were excluded from our study (we note, however, that the image quality of VISIR prior to its upgrade was extensively studied in Reference 4, with similar results as the ones shown here).

Fig. 1 shows the achieved IQ (taken as the average FWHM of all four beams; the error bars indicate the spread in these values) as a function of airmass in each VISIR imaging filter. Also shown in each panel are curves

*<http://www.eso.org/observing/etc>

†<http://www.eso.org/observing/dfo/quality/VISIR/qc/qc1.html>

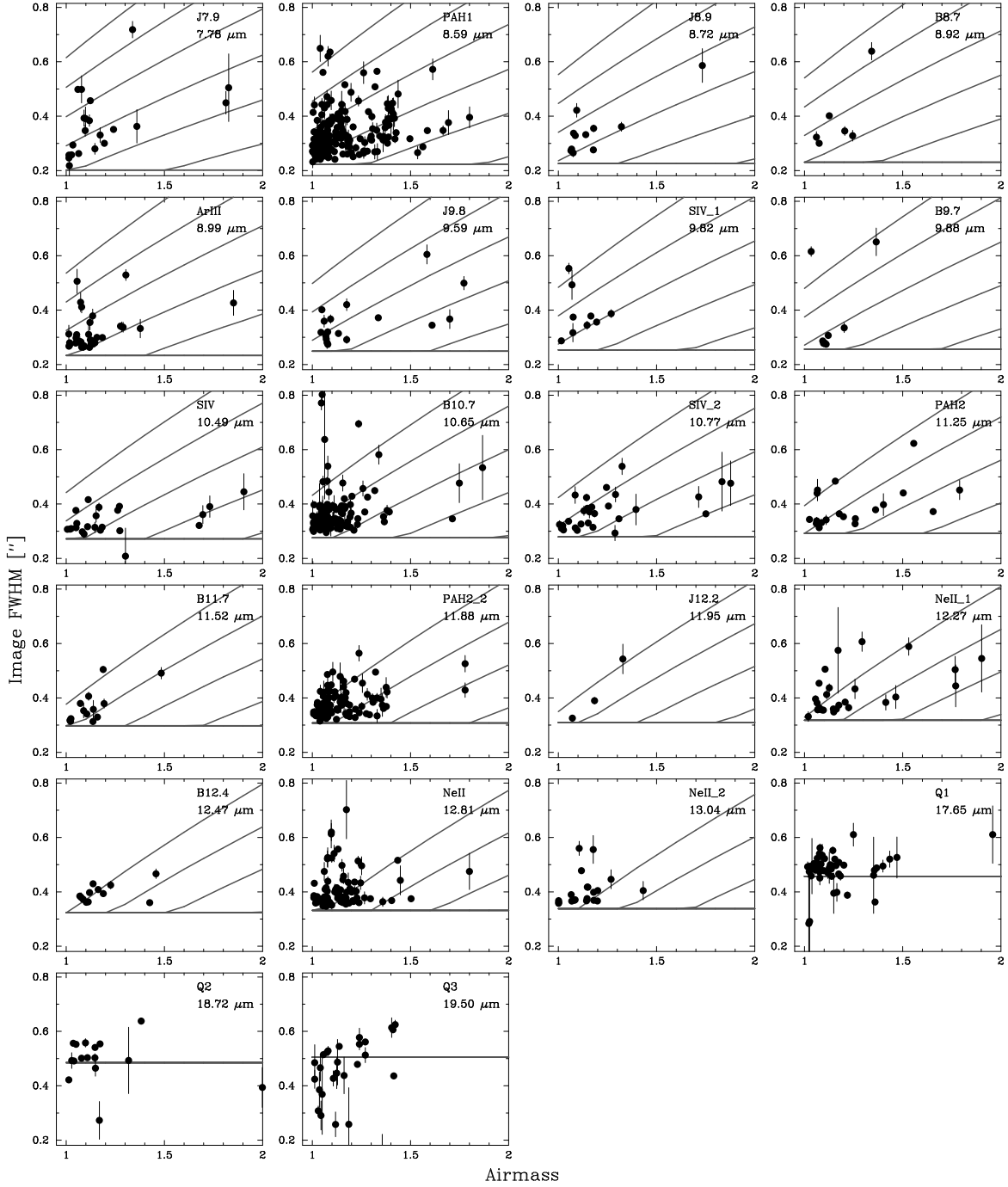


Figure 3. Achieved Image Quality as a function of airmass for VISIR standard stars observed between March 1 and October 20, 2015. In each plot the lines show the predicted behaviour for an optical seeing of (from top to bottom) 2.0, 1.8, 1.6, 1.4, 1.2, 1.0, 0.8, 0.6, and 0.4" using the modified form of the ETC formula with $FWHM_{atm} \propto \lambda^{-0.1}$.

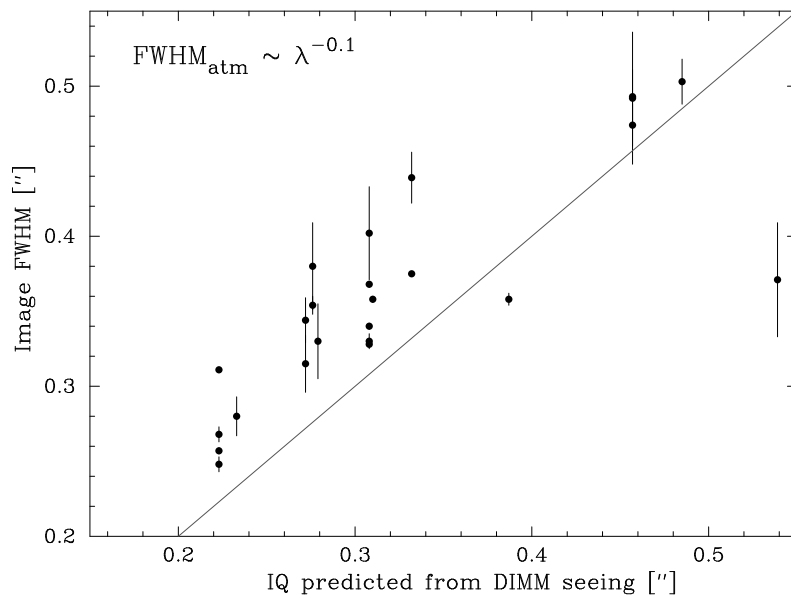
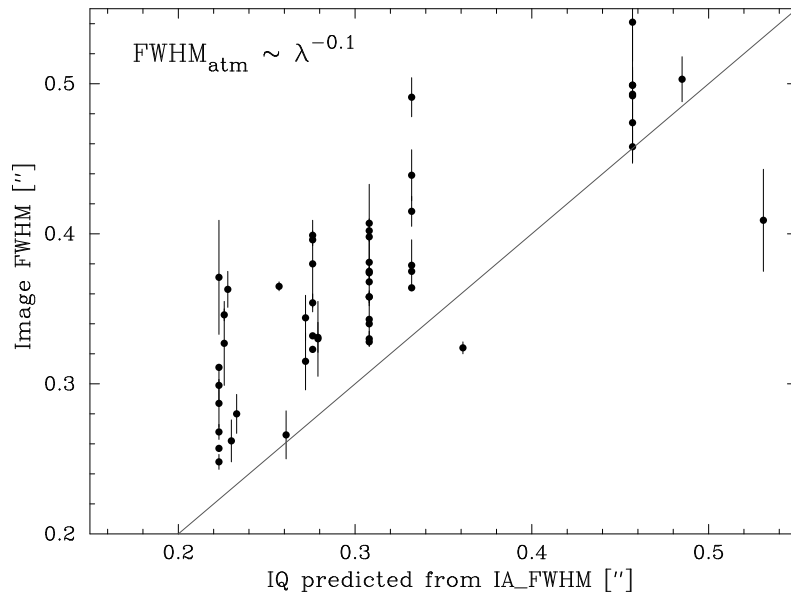


Figure 4. Comparison of achieved versus predicted image quality using IA_FWHM (“telescope” seeing) (top) and predicted image quality versus DIMM seeing (bottom) using the modified form of the ETC formula with $FWHM_{atm} \propto \lambda^{-0.1}$. The solid line indicates achieved IQ = predicted IQ.

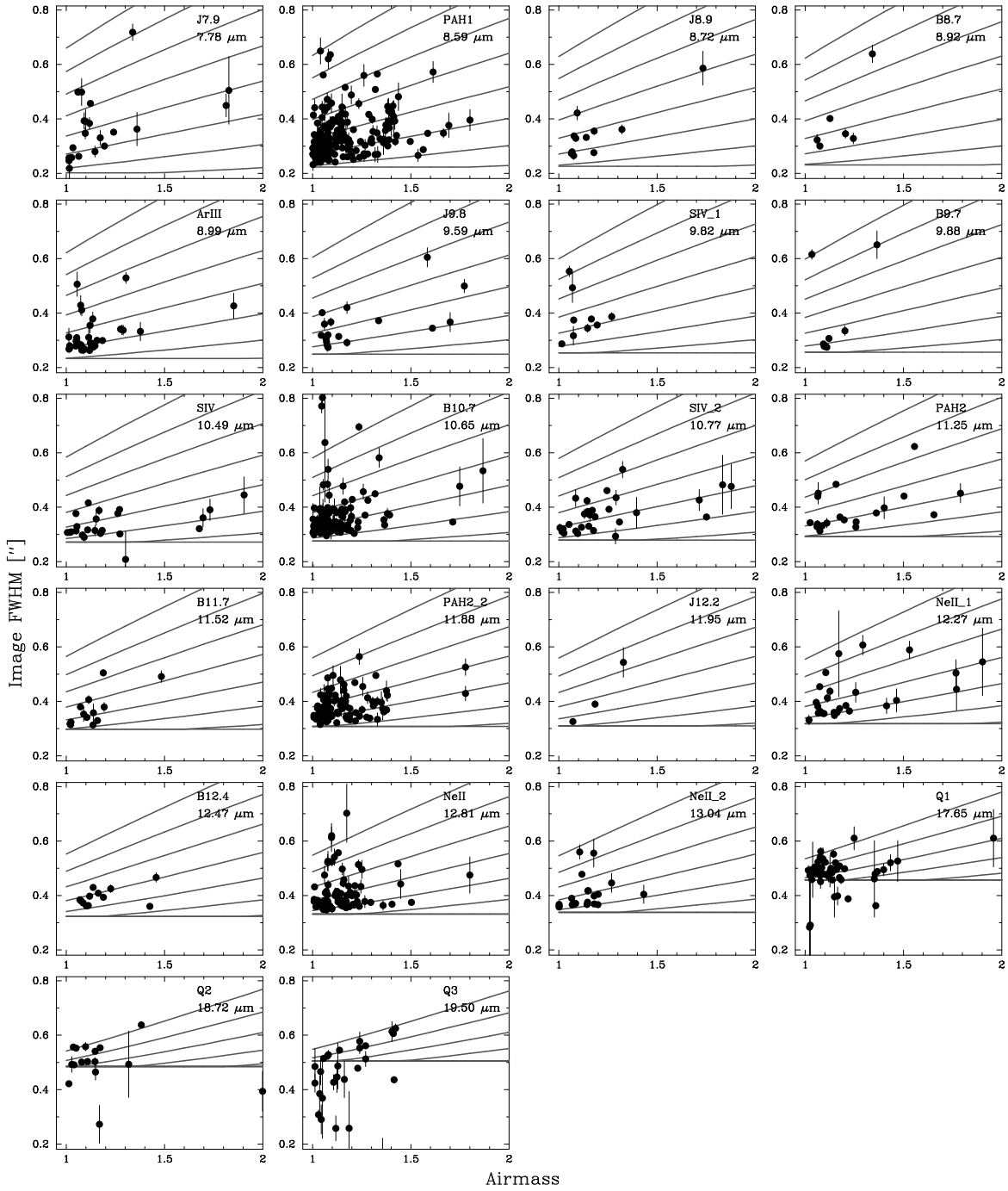


Figure 5. Achieved Image Quality as a function of airmass for VISIR standard stars observed between March 1 and October 20, 2015. In each plot the lines show the predicted behaviour for an optical seeing of (from top to bottom) 2.0, 1.8, 1.6, 1.4, 1.2, 1.0, 0.8, 0.6, and 0.4" using $L_0 = 46$ m.

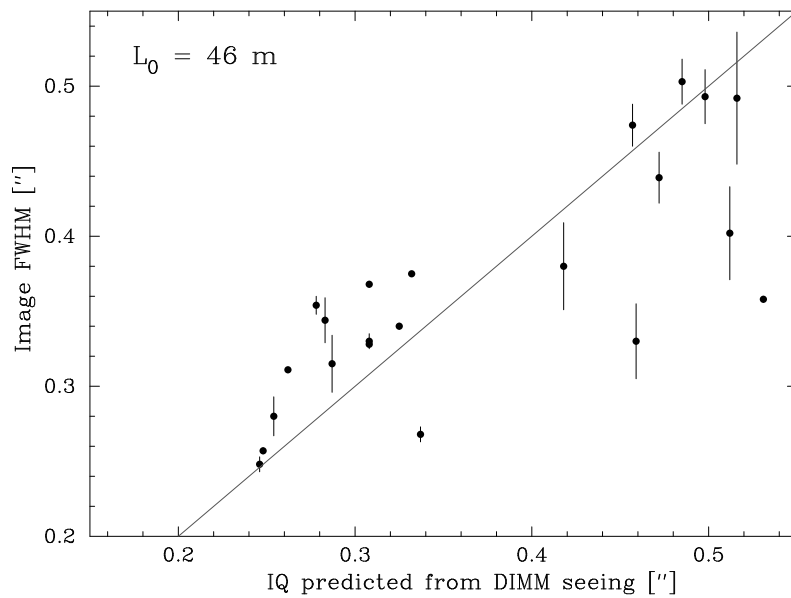
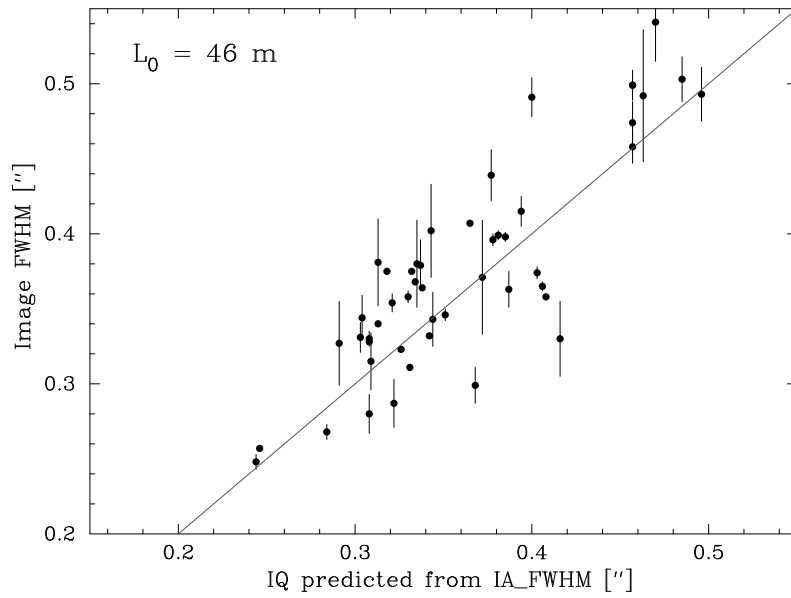


Figure 6. Comparison of achieved versus predicted image quality using IA_FWHM ("telescope" seeing) (top) and predicted image quality versus DIMM seeing (bottom) using $L_0 = 46$ m. The solid line indicates achieved IQ = predicted IQ.

Table 1. Comparison of predicted image quality using modified versions of the ETC formula. Airmass has been kept fixed at 1.2 for all computations.

Band	λ [μm]	Original formula				$FWHM_{atm} \propto \lambda^{-0.1}$				$L_0 = 46 \text{ m}$			
		0.4''	0.8''	1.2''	1.6''	0.4''	0.8''	1.2''	1.6''	0.4''	0.8''	1.2''	1.6''
U	0.37	0.379	0.804	1.237	1.676	0.367	0.779	1.199	1.624	0.401	0.837	1.279	1.726
B	0.44	0.358	0.764	1.179	1.600	0.353	0.753	1.163	1.578	0.381	0.799	1.224	1.653
V	0.55	0.330	0.713	1.105	1.503	0.333	0.719	1.115	1.517	0.356	0.751	1.153	1.559
R	0.63	0.313	0.681	1.059	1.442	0.320	0.697	1.084	1.477	0.340	0.720	1.108	1.501
I	0.88	0.274	0.610	0.958	1.311	0.290	0.646	1.013	1.387	0.305	0.654	1.013	1.376
J	1.22	0.235	0.541	0.859	1.183	0.257	0.591	0.939	1.294	0.271	0.591	0.921	1.255
H	1.63	0.201	0.480	0.773	1.073	0.225	0.540	0.869	1.207	0.242	0.536	0.841	1.152
K	2.19	0.165	0.418	0.686	0.961	0.188	0.483	0.794	1.114	0.213	0.481	0.762	1.050
L	3.45	0.112	0.320	0.551	0.790	0.121	0.383	0.665	0.957	0.176	0.400	0.645	0.898
M	4.75	0.123	0.251	0.454	0.669	0.123	0.300	0.561	0.833	0.163	0.349	0.566	0.794
J7.8	7.78	0.202	0.202	0.307	0.479	0.202	0.202	0.365	0.607	0.202	0.293	0.458	0.644
J8.9	8.72	0.226	0.226	0.276	0.436	0.226	0.226	0.309	0.545	0.226	0.290	0.438	0.613
J9.8	9.59	0.249	0.249	0.253	0.401	0.249	0.249	0.257	0.490	0.249	0.291	0.424	0.589
J12.2	11.95	0.310	0.310	0.310	0.327	0.310	0.310	0.310	0.342	0.310	0.311	0.406	0.542
Q1	17.65	0.457	0.457	0.457	0.457	0.457	0.457	0.457	0.457	0.457	0.457	0.457	0.520
Q2	18.72	0.485	0.485	0.485	0.485	0.485	0.485	0.485	0.485	0.485	0.485	0.485	0.527
Q3	19.50	0.505	0.505	0.505	0.505	0.505	0.505	0.505	0.505	0.505	0.505	0.505	0.534

showing the predictions from the equations by Martinez et al. (Section 2), for an optical seeing (from top to bottom) of 2.0, 1.8, 1.6, 1.4, 1.2, 1.0, 0.8, 0.6, and 0.4''. As can be seen from Fig. 1 in the N -band (7-13 μm) the achieved image quality is always larger than the one predicted for median (0.8-1.0'') optical seeing conditions, i.e. *the formula used to extrapolate optical to mid-IR seeing systematically predicts a better IQ than is achieved in the mid-IR*. For the Q -band filters the achieved image quality is close to the predictions (which are dominated by the telescope diffraction limit), so we conclude that in the Q -band seeing indeed does not greatly contribute to image quality.

The effect noted above can also be seen when directly plotting the achieved versus predicted image quality using the optical seeing from the QC1 database (Fig. 2). Whereas for predicted IQ $> 0.4''$ (corresponding to Q -band data), the agreement between the two is acceptable, for IQ predictions smaller than 0.4'' (N -band) the measured IQ is consistently $\sim 0.1''$ worse than predicted by the equations listed in Section 2.

4. ANALYSIS OF DIFFERENCES BETWEEN PREDICTED AND ACHIEVED IQ

In the last section we saw that the equations given in Section 2 systematically predict a better IQ in the N band than the IQ achieved by VISIR. The fact that the IQ achieved by VISIR in Q is close to the diffraction limit of the telescope, strongly suggests that this behaviour is not due to the transfer function of the instrument, but must be caused by the term in equation (1) due to image degradation by the earth's atmosphere. Further evidence that this indeed comes from the effect of the atmosphere comes from the observation that the lower envelope of the data points shown in Fig. 1 indeed follows the $x^{0.6}$ dependence on airmass predicted by equation (2).

Analyzing the equations given in Section 2 we notice there are two mathematical options to change the wavelength dependence of these equations: (a) change the exponent of the wavelength term in equation (2), (b) change the wavelength-dependence of the square-root term in equation (2). We investigate the following two possibilities: (1) adopting $FWHM_{atm} \propto \lambda^{-0.1}$ instead of the $FWHM_{atm} \propto \lambda^{-0.2}$ wavelength dependence used in equation (2), and (2) adopting $L_0 = 46 \text{ m}$ instead of the canonical value of 23 m.[‡]

[‡]We note that changing other factors in the square-root term in equation (2), such as modifying $F_{K_{olb}}$ instead of L_0 can provide mathematically identical results. As empirically one cannot distinguish between these possibilities we will only focus on varying L_0 here.

Figs. 3–6 present the results of the comparison of the measured image quality with the modified forms of the ETC equations. From Figs. 3 and 4 it is apparent that although the agreement between model prediction and measured image quality improves when adapting $FWHM_{atm} \propto \lambda^{-0.1}$, the model still predicts a somewhat better image quality in the N -band than is realized. In addition, the model predictions at optical and near-IR wavelengths may start to deviate significantly from the original model when adopting this change in wavelength dependence (Table 1). Therefore it seems unlikely that a change in power-law index alone can fully describe the observed wavelength-dependence of atmospheric blurring of stellar images.

In contrast to this, we find a satisfactory match between model prediction and observed VISIR image quality when adopting $L_0 = 46$ m (Figs. 5 and 6), whereas this change only has moderate effects on the predicted image quality in the optical and near-IR. We note that not all values in Fig. 6 match within their error bars with the model prediction based on either FWHM_{IA}, or the DIMM seeing. As already speculated upon in the paper in which this formula was first derived,¹ this may indicate that L_0 may in fact vary depending on the actual atmospheric conditions, so the wavelength-dependence of the seeing may not be purely described by the free parameters x and s in equation (2), but to some degree L_0 may also be a free parameter. For the purpose of these proceedings we will ignore this subtlety and we pose that $L_0 = 46$ m provides a better description for the median conditions of the atmosphere on Paranal than the so far adopted value of 23 m.

5. CONCLUSIONS

The analysis presented in the previous sections showed that there is a systematic difference of about 0.1” between the N -band image quality predictions of the VISIR ETC based on the optical seeing and the realized image quality. The fact that (1) measured image quality is not constant, (2) the image quality achieved by VISIR in the N -band is close to that achieved by other mid-IR instruments on 8-m class telescopes,⁵ (3) in the Q -band measured image quality is indeed close to the diffraction limit, and (4) image quality in the N -band shows the expected $x^{0.6}$ dependence on airmass shows that this difference is due to the effects of the earth’s atmosphere and not due to image degradation within the instrument.

This difference in predicted and achieved image quality has important implications for the scheduling of VISIR service-mode observations, as a simplified form of the equations listed in Section 2 is implemented within ESO’s Observing Tool (OT), where it is used for the filtering of observable OBs based on the image constraint given in each observing block, and the expected image quality based on the airmass of the target and the optical seeing. The systematic under-estimation of the actually achievable mid-IR image quality based on optical seeing noted here may lead to some observations in service-mode being executed out of their constraints and having to be repeated to yield the date quality requested by the PI.

We also investigated two possibilities to align the predictions of the equations used to extrapolate optical to mid-IR seeing with the measurements, by either adopting a wavelength-dependence $\lambda \propto \lambda^{-0.1}$ (instead of the current $\lambda \propto \lambda^{-0.2}$), or by adopting an outer length-scale of the atmospheric turbulence $L_0 = 46$ m (instead of the currently used $L_0 = 23$ m).[§] Either option improves the agreement between predicted and achieved image quality in the mid-IR, but only changing L_0 provides better agreement between predicted and observed image quality in the N -band while maintaining nearly the same predicted image quality in the optical and near-IR. We therefore recommend the latter option to be adopted for use in science operations with VISIR.

REFERENCES

- [1] Martinez, P., Kolb, J., Sarazin, M., and Tokovinin, A., “On the Difference between Seeing and Image Quality: When the Turbulence Outer Scale Enters the Game,” *The Messenger* **141**, 5–8 (Sept. 2010).
- [2] Kerber, F., Käuff, H. U., Baksai, P., Dobrzycka, D., Finger, G., Ives, D., Jakob, G., Lagadec, E., Lundin, L., Mawet, D., Mehrgan, L., Moerchen, M., Momany, Y., Moreau, V., Pantin, E., Riquelme, M., Siebenmorgen, R., Silber, A., Smette, A., Taylor, J., van den Ancker, M., Venema, L., Weilenmann, U., and Yegorova, I.,

[§]We again stress that changing other factors within the square-root term in Equation (2), such as modifying $F_{K_{ob}}$ will produce mathematically identical results to the change in L_0 we propose here. Empirically we cannot determine which option would correspond more accurately to the actual physical state of the atmosphere.

- “VISIR upgrade overview and status,” in [*Ground-based and Airborne Instrumentation for Astronomy IV*], *Proceedings of the SPIE* **8446**, 84460E (Sept. 2012).
- [3] Kerber, F., Käußl, H.-U., Baksai, P., Di Lieto, N., Dobrzycka, D., Duhoux, P., Finger, G., Heikamp, S., Ives, D., Jakob, G., Lundin, L., Mawet, D., Mehrgan, L., Momany, Y., Moreau, V., Pantin, E., Riquelme, M., Sandrock, S., Siebenmorgen, R., Smette, A., Taylor, J., van den Ancker, M., Valdes, G., Venema, L., and Weilenmann, U., “VISIR upgrade overview and status,” in [*Ground-based and Airborne Instrumentation for Astronomy V*], *Proceedings of the SPIE* **9147**, 91470C (July 2014).
- [4] Verhoeff, A., *Dusty Disks around Young Stars*, PhD thesis, Sterrenkundig Instituut ”Anton Pannekoek”, University of Amsterdam (Nov. 2009).
- [5] Mason, R., Wong, A., Geballe, T., Volk, K., Hayward, T., Dillman, M., Fisher, R. S., and Radomski, J., “Observing conditions and mid-IR data quality,” in [*Observatory Operations: Strategies, Processes, and Systems II*], *Proceedings of the SPIE* **7016**, 70161Y (July 2008).